J Solid State Electrochem (2009) 13:1859–1865
DOI 10.1007/s10008-008-0737-6

ORIGINAL PAPER

Fitting of the voltage–Li^+ insertion curve of $LiFePO_4$

Mauro Pasquali · Alessandro Dell'Era · Pier Paolo Prosini

Received: 22 February 2008 / Revised: 19 September 2008 / Accepted: 8 November 2008 / Published online: 9 December 2008

Abstract Fitting of the voltage vs. insertion curves of the $LiFePO_4$ electrode was based on theoretical expressions describing the Li^+ diffusive process in a solid medium. The noninteracting gas model for the chemical potential of ions distributed in a solid matrix was taken into account, and the diffusion coefficient and the energy activation for the diffusion process were accordingly calculated. The polarization curves at various discharge stages were theoretically obtained, and a good agreement was found with the experimental data at all discharge rates. A mathematical relation describing the trend of the diffusion resistance vs. insertion degree was also developed.

Keywords Lithium iron phosphate · Discharge curves simulation · Diffusivity · Diffusion resistance · Noninteracting gas model

Introduction

Lithium iron phosphate is a very interesting positive electrode for low-cost, high-energy lithium-ion batteries [1–5]. A critical factor for its electrochemical performance is represented by the low electronic conductivity [6]. The lithium ion's jump from one site to another requires a simultaneous passage of electrons between sites. Therefore, if the ionic conductivity of the material is higher than the electronic one, the ionic diffusivity is limited by the low electronic diffusivity. In the opposite case, the electronic conductivity is limited by the lower ionic diffusivity, and the grain size is important for obtaining a good electrochemical performance. In this work, it is assumed that the ionic diffusivity is the kinetic critical factor for a high performance and that the chemical potential of the $LiFePO_4/FePO_4$ couple is essentially uniform throughout the materials. Only ionic transport will be considered for the discussion.

It is important to specify that Li^+ insertion/deinsertion in $LiFePO_4$ is accompanied by strong electron–ion interactions leading to the coexistence of two phases. Therefore, the insertion process proceeds by one or several reaction fronts and, in principle, is incorrect to define a diffusion coefficient. However, McKinnon and Hearing found that it is not possible to distinguish between two different diffusion models based on continuous (solid solution formation) or noncontinuous (two-phase formation) processes of Li^+ uptake or removal [7]. Based on this assumption, the term diffusion coefficient, D, will be used in this work too.

$LiFePO_4$ preparation

Fe(II) methyl phosphonate $Fe((CH_3PO_3)(H_2O))$ (FeMP) and Fe(II) phenyl phosphonate $Fe((C_6H_5PO_3)(H_2O))$ (FePP), the precursors of $LiFePO_4$, have been synthesized as reported in [8]. These compounds can be isolated as white microcrystalline powders and are stable in the air. Li_2CO_3 and FeMP or FePP (1:2 ratio) were ball-milled to get an intimate mixture. Gray powders of $LiFePO_4$ were obtained by heating the precursor mixtures in a tubular furnace under N_2 at temperatures above 600°C for at least 16 h.

M. Pasquali · A. Dell'Era (✉)
Department of Chemical Engineering,
University of Rome "La Sapienza",
via del Castro Laurenziano 7,
00184 Rome, Italy
e-mail: alessandro.dellera@uniroma1.it

P. P. Prosini
ENEA IDROCOMB, C.R. Casaccia,
Santa Maria di Galeria, 00060 Rome, Italy

Experimental system

The electrodes used for the electrochemical characterization were prepared by mixing 10 mg of $LiFePO_4$ powder with 10% carbon and 5% teflon. The cathode components were pestled in a mortar and laminated. Electrodes with a surface "*a*" of ~1 cm^2 were punched from the foil. Then, the electrodes were placed in a cell also containing Li foils (as anode and reference electrodes), a glass wool separator and 1 M $LiPF_6$–DMC:EC (1:1) as electrolyte. The same configuration was used for electrochemical impedance spectroscopy (EIS) and potentiostatic–intermittent titration technique (PITT) experiments.

A frequency response analyzer (Solartron 1255 HF and Solartron 1286 models by EG & G) and a galvanostat–potentiostat (Mac-Pile II Biologic) were used for these experiments.

Discussion

The chemical potential is a function of the ions distributed in the sites of a solid matrix and takes the form [8]:

$$\mu(x) = E_0 + k_B T \ln\left(\frac{x}{1-x}\right) \tag{1}$$

where E_0 is the energy of the sites.

The diffusion resistance, R, is defined as [8]:

$$R(x) = \frac{L^2}{D \cdot \overline{V} e^2 N \frac{dx}{d\mu}} \tag{2}$$

In the quasi-equilibrium approximation, the diffusion coefficient, D, is defined as [8]:

$$D(x) = \frac{D_J(x)}{k_B T} x \frac{d\mu}{dx} \tag{3}$$

where D_J is the kinetic or jump diffusion coefficient:

$$D_J(x) = \frac{M_0}{x} \exp\left(-\frac{E_a}{RT}\right) P(0;0) \tag{4}$$

P(0;0) is the probability for two nearest neighbor lattice sites to be vacant [8, 9]. For noninteracting lattice gases $P(0;0) = (1-x)^2$ and E_a is the activation energy/mol [10, 11]. Finally, the diffusion resistance assumes the form (used for the fit):

$$R(x) = \frac{L^2}{D(x)\overline{V} e^2 N \frac{dx}{d\mu}} = \frac{L^2 k_B T}{D_J(x)\overline{V} e^2 N x} = \frac{L^2 k_B T}{\overline{V} e^2 N M_0 \exp\left(-\frac{E_a}{RT}\right)(1-x)^2} \tag{5}$$

Electrochemical parameters determination

To determine the diffusion resistance, expression 6 was used. It represents a polarization curve and includes the exchange current density, i_o, the Tafel slope, b, and the electrolyte resistance, R_e. Therefore, these electrochemical parameters were firstly measured by EIS in a three-electrode cell.

$$E = E^o(x) - b \ln(i/i_o) - (R_e + R(x)) \cdot i \cdot a \tag{6}$$

The exchange current density is related, by Eq. 7, to the charge transfer resistance that can be obtained from the Nyquist diagram (Fig. 1) as the difference between the second and first intercept of the semicircle with the abscissa. R_{ct} was found to be equal to ~85 Ω.

Therefore, from the following relation, valid for very low over-voltage values [12–14]:

$$i_o \cdot a = \frac{\overline{R}T}{\overline{n}FR_{ct}} \tag{7}$$

i_o at 20°C can be obtained:

$$i_o = 2.9 \times 10^{-4} \mathrm{A/cm^2} \tag{8}$$

Then, the b value may be calculated from the following relation:

$$b = \frac{\overline{R}T}{\overline{n}F\alpha} = 0.05\mathrm{V} \tag{9}$$

where α is the transfer coefficient (normally assumed equal to 0.5).

The exchange current density was also measured by a Tafel plot and a cyclic voltammetry curve (Figs. 2 and 3,

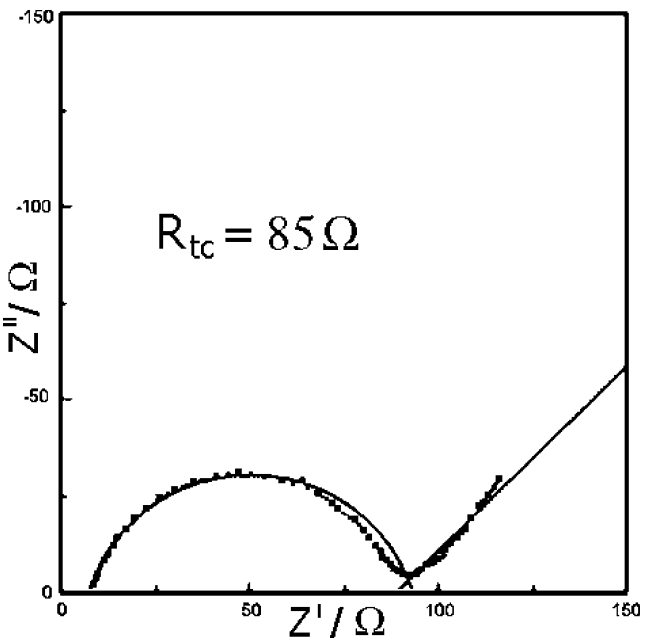

Fig. 1 Nyquist plot

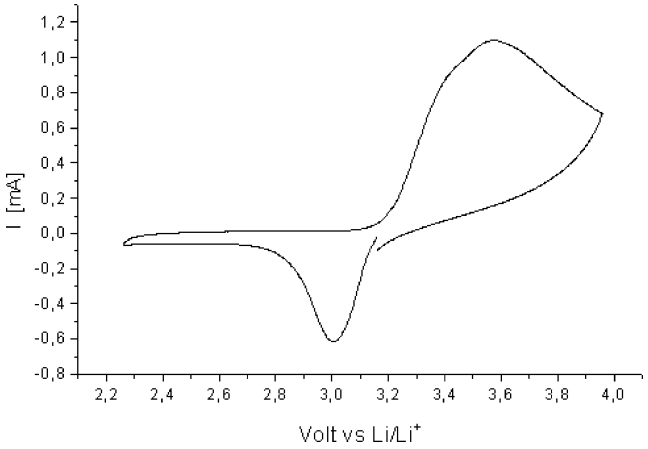

Fig. 2 Tafel curve

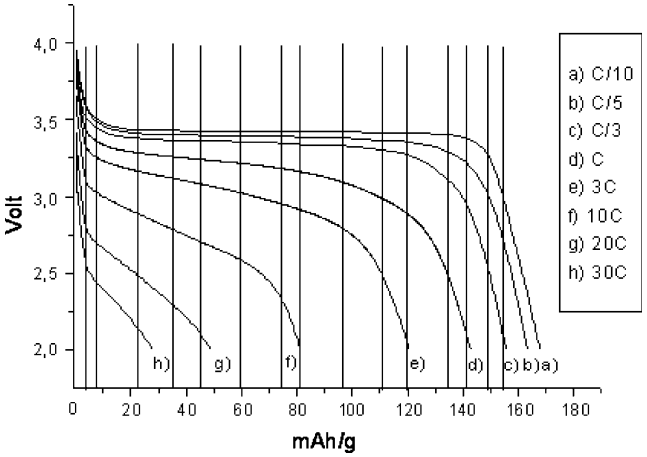

Fig. 4 Discharge curves

respectively). The value of i_o so determined is somewhat smaller than that of expression 8:

$$i_o = 1.3 \times 10^{-4} \mathrm{A/cm^2}$$

As the geometric surface was used in the calculation, the i_o values are a characteristic of the electrode rather than of the active material.

The electrolyte resistance, R_e, was determined from the value of the first intercept of the semicircle of Fig. 1; it is equal to ~8 Ω.

An E^o=~3.45 V can be derived for $LiFePO_4$. Figure 4 reports the discharge curves at various rates for an electrode containing ~10 mg of $LiFePO_4$. Using these curves, the polarization curves of Figs. 5, 6, 7, and 8 could be drawn. Each polarization curve corresponds to a fixed insertion degree (mAh/g) related to every single vertical segment of Fig. 4.

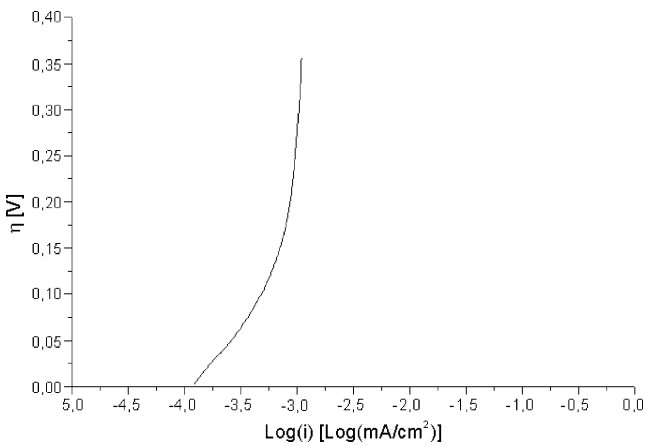

Fig. 3 CYclic voltammetry at 0.5 mV/s of a de-litiated electrode

Diffusion resistance determination

At this point, in expression 6, only the diffusion resistance remains to be determined. Therefore, by fitting the polarization curves, the diffusion resistance was obtained as a function of the insertion degree, as shown in Fig. 9.

The diffusion resistance increases with the insertion degree, the highest value being observed near total discharge. To fit the experimental data, a function similar to Eq. 5 was looked for and the following expression (Eq. 10):

$$R = \frac{A}{\exp(-B)(1-x)^2} \tag{10}$$

was found to fit very well the data if coefficients A and B have the values:

$$A = 1.3 \times 10^{-6} \mathrm{ohm}; \quad B = 15.85$$

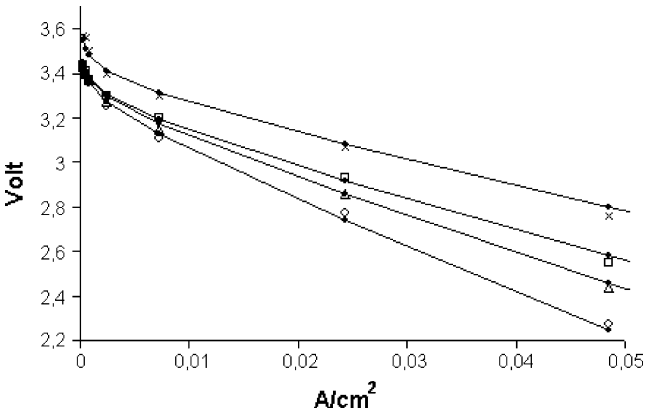

Fig. 5 Polarization curves fitting: (*ex sign*) 4.4 mAh/g; (*empty square*) 17.7 mAh/g; (*empty triangle*) 24. 2 mAh/g; (*empty diamond*) 35. 5 mAh/g

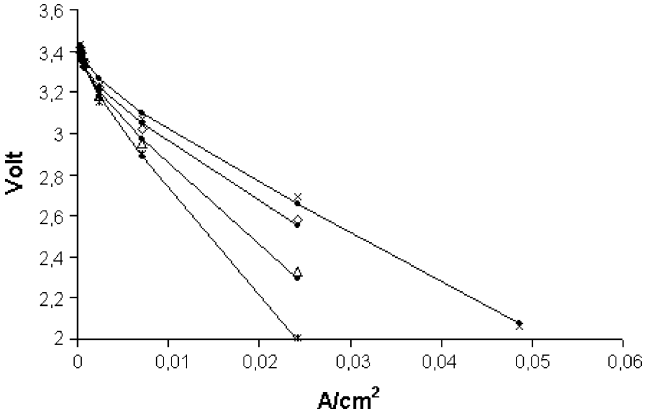

Fig. 6 Polarization curves fitting: (*ex sign*) 46. 3 mAh/g; (*empty square*) 58. 8 mAh/g; (*empty triangle*) 73.8 mAh/g; (*asterisk*) 80. 9 mAh/g

Let us consider now expression 1. The term $\left(\frac{\partial x}{\partial \mu}\right)$ may be obtained, which is given by:

$$\left(\frac{\partial x}{\partial \mu}\right) = \frac{x(1-x)}{k_B T}$$

By putting it into Eq. 5, $R(x)$ may be written as:

$$R(x) = \frac{L^2}{D(x)\overline{V}e^2 N \frac{dx}{d\mu}} \tag{11}$$

For x=0.5, assuming T=293.15 K, the specific capacity of $LiFePO_4$ as 0.17 Ah/g or 612 C/g, the density of $LiFePO_4$ as 3.9 g/cm^3, the charge density "$N\times e$" for $LiFePO_4$ is equal to: 612·3.9=2,386.8 C/cm^3 or 2.386×

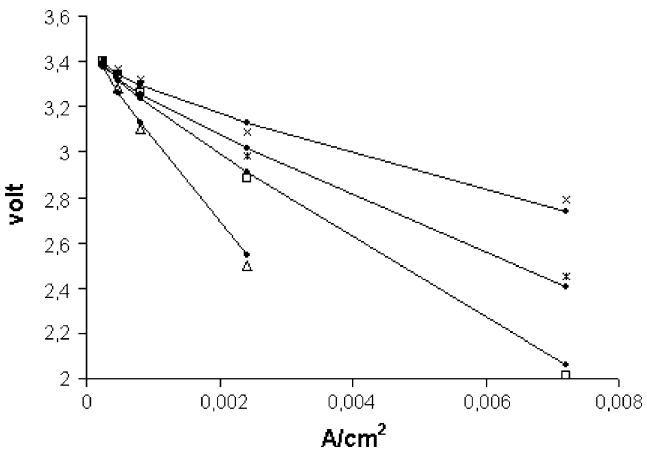

Fig. 7 Polarization curves fitting: (*ex sign*) 96. 4 mAh/g; (*asterisk*) 111. 3 mAh/g; (*empty square*) 120 mAh/g; (*empty triangle*) 134 mAh/g

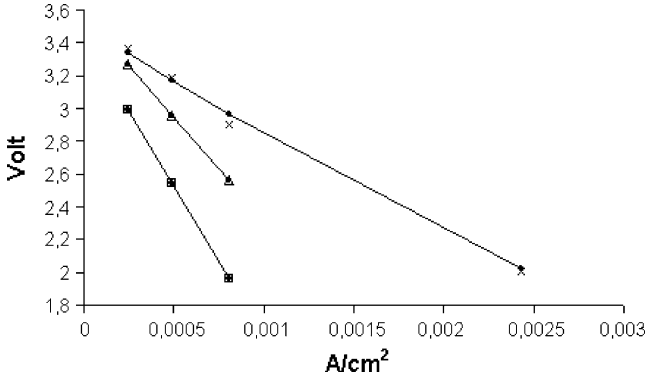

Fig. 8 Polarization curves fitting: (*ex sign*) 141. 8 mAh/g; (*empty triangle*) 148 mAh/g; (*empty square*) 155 mAh/g

10^9 C/m^3. Assuming that the active material volume $\overline{V}$, in our experiments, is:

$$\frac{1}{3.9} \times 0.01 = 2.56 \times 10^{-3} \left[\frac{\text{cm}^3}{g}\right] \cdot [g]$$

or: 2.56×10^{-9} m^3,expression 11 becomes:

$$R(0.5) = \frac{1.38 \times 10^{-23} \times 293.15 \times L^2}{2.56 \times 10^{-9} \times 1.6022 \times 10^{-19} \times 2.386 \times 10^9 \times 0.25 \times D(0.5)} = 38\Omega$$

$$R(0.5) = \frac{0.0165 \times L^2}{D(0.5)} = 38\Omega \tag{12}$$

As a final assumption, the characteristic diffusion length (L) was set equal to the radius of the particle, L. The latter was estimated as ~0.1×10^{-4} cm (Fig. 10). Therefore, a value

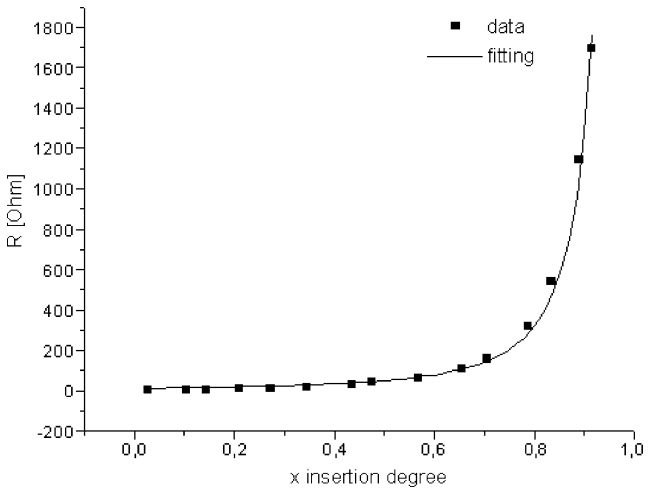

Fig. 9 (*filled square*) Diffusion resistance vs. insertion degree; (*straight line*) Diffusion resistance fitting

4.3×10^{-14} cm^2/s was calculated for the diffusion coefficient, which is very close to the values reported in [1, 15, 16].

Experimental determination of the activation energy for Li^+ insertion

By the fit, E_a results to be:

$$E_a = 15.85 \times \overline{R} \times T = 15.85 \times 8.31 \times 293.15 \cong 38.6 \text{ kJ/mol}. \quad (13)$$

This value is an excellent agreement with the one reported in [9] (39 kJ/mol^{-1}). To confirm the validity of the fitting, the activation energy has been also calculated for x=0.25 and x=0.75.

Using expressions 1, 3, and 4, D is:

$$D = M_0\left(\frac{1-x}{x}\right)\exp\left(-\frac{E_a}{\overline{R}T}\right) \quad (14)$$

and

$$\ln D = \ln\left(M_0\frac{1-x}{x}\right) - \frac{E_a}{\overline{R}T} \quad (15)$$

The diffusion coefficient of $LiFePO_4$ has been calculated using the potential step cyclic voltammetry (PITT technique, Table 1) at different temperatures on the first sweep oxidation peak [from 3.25 V (open circuit voltage) to 4 V (final voltage)]. In all experiments, the open circuit relaxation time was 20 s and the step duration 10 s if I_o< 0.01 mA.

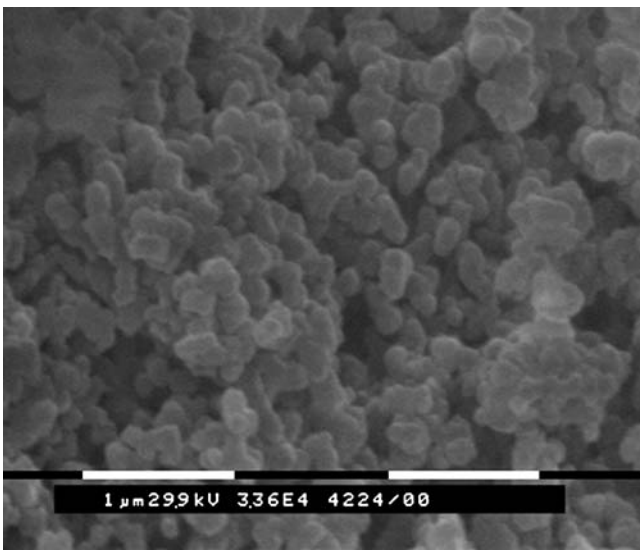

Fig. 10 SEM picture of $LiFePO_4$

Table 1 Cottrell parameter

Method	Cottrell parameter	Value
PITT and Cottrell region	log (Λ)	2
PITT and Cottrell region	D_{ap}/D	1

Plotting $I\sqrt{t}$ vs. log(t), where I is the current value during the potential step at 3.43 V (x=0.25) and 3.46 V (x=0.75; when the current value is very low as in voltammetry experiments, $LiFePO_4$ de-intercalates almost all the charge within the voltage range 3.42–3.47 V), it is possible to specify a particular region where $I\sqrt{t}$ is almost constant and to highlight a Cottrell behavior.

As stressed in [17], the diffusion coefficient, calculated determining the Cottrell region, can be often underestimated; to calculate the real diffusion coefficient, it is necessary to evaluate the dimensionless parameter Λ, defined as [18–19]:

$$\Lambda = \frac{R_d}{R_\Omega + R_{ct}} \quad (16)$$

where R_d is the diffusion resistance, R_Ω the ohmic resistance, and R_{ct} the charge transfer resistance. For $LiFePO_4$, log (Λ)=2 (see Table 1), and in this condition, the following expression (Eq. 17) is valid within the Cottrell region [20, 21]:

$$I(t)\sqrt{t} = \frac{QD^{1/2}}{L\pi^{1/2}} = \text{constant} \quad (17)$$

where Q is the charge intercalated during the step, L is the characteristic diffusion length, I is the current during the step, and D is the real diffusion coefficient; knowing the first three parameters, it is possible to calculate the last one. Therefore, plotting ln(D) as a function of $\frac{1}{T}$ and determining the slopes of the straight lines (Fig. 11), the activation energies may be calculated (Table 2). In both cases, the activation energy values are very similar to the experimental and fitted ones at x=0.5 [9].

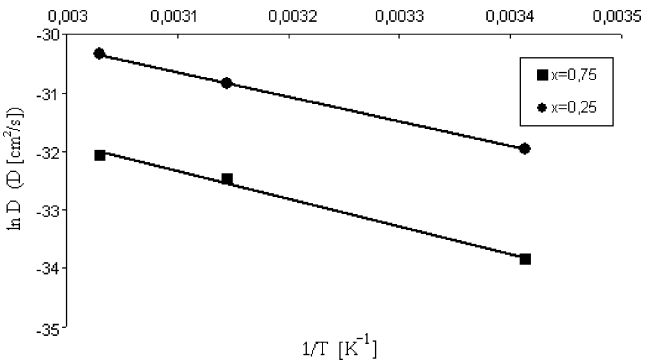

Fig. 11 Diffusivity coefficient as a function of 1/T in logarithmic scale (*filled dots*) for x=0.25 and (*filled squares*) x=0.75

Table 2 Activation energy for the diffusion process at x=0.25 and x=0.75

Insertion degree "x"	Activation energy (kJ/mol)
0.25	35.0
0.75	39.6

Fitting of the discharge curves

Finally, for the first term of expression 6, a logistic function has been used [22]. We assume that when the discharge begins and Li ions are accepted into the $FePO_4$ structure, they firstly occupy all sites of more external shells. As soon as this first filling is complete, a new phase ($LiFePO_4$) forms within this shell that grows step-by-step inside the active material. It is supposed that during this primary filling of $FePO_4$ the $E°(x)$ voltage changes according to a curve described by a logistic function quite similar to the one we propose. Therefore expression 6 becomes:

$$E(x) = \left[\frac{(E_{ec} - \overline{E})}{(1 + \frac{x}{\overline{x}})} + \overline{E}\right] - b\ln(i/i_o) - \left[R_e + \frac{A}{\exp(-B)(1-x)^2}\right] \times i \times a \qquad (18)$$

where E_{ec} is the voltage at the end of charge (in this case, 4 V), $\overline{E}$ is the voltage near reversibility conditions, and $\overline{x}$ is the insertion degree corresponding to the mean voltage difference $(E_{ec} - \overline{E})$. In the above equation, the second term of the right-hand member is the barrier overpotential, the third term is the ohmic electrolyte resistance R_e, and the last term is the diffusion overpotential. Finally, Figs. 12 and 13 show the fitting of the $LiFePO_4$ discharge curves for various discharge rates using such relation.

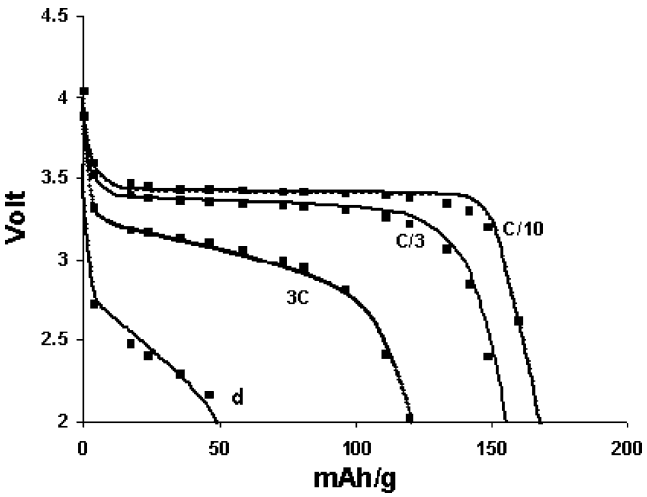

Fig. 12 Discharge curves fitting at **a** C/10, **b** C/3, **c** 3C, **d** 20C; (*filled square*) fit

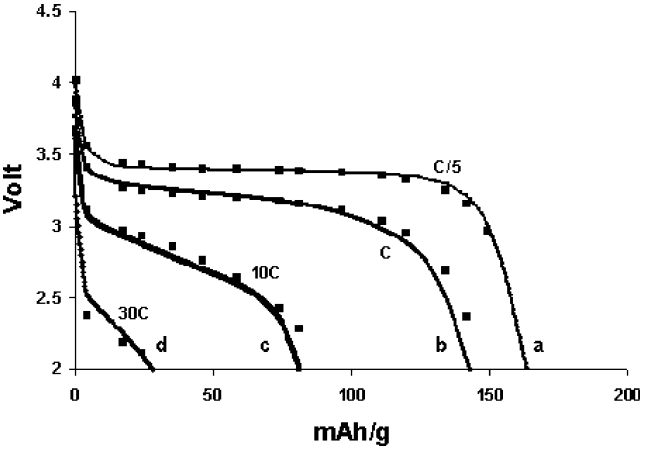

Fig. 13 Discharge curves fitting at **a** C/5, **b** C, **c** 10C, **d** 30C; (*filled square*) fit

Conclusion

Some authors have tried to fit the discharge curves of $LiFePO_4$, but even if the fitting was quite close to the real curves, a good agreement at all rates could not be observed. In this work, polarization curves for various discharge stages were theoretically obtained, and a good agreement was found with experimental data also at high discharge rates. A mathematical relation describing the trend of the diffusion resistance vs. insertion degree was also developed. The values of the diffusivity, assuming a noninteracting gas model, and of the activation energy have been also determined. The values obtained are in good agreement with the ones reported in the literature. The method presented in this work can be used to find an expression able to predict the behavior of other cathode materials during charge or discharge.

Nomenclature

M_0	Ionic mobility coefficient (cm^2/s)
L	characteristic diffusion length (cm)
e	positive elementary charge=1.6022×10^{-19} (C)
n	number density of intercalated atoms
N	number density proportional to the size of the host
$\overline{V}$	active material volume (m^3)
k_B	Boltzmann constant $= 1.38 \times 10^{-23}\left[\frac{J}{K}\right]$
T	temperature (K)
C	capacitance (F)
Q	charge (C)
$\overline{R}$	gas constant $\left[\frac{J}{K\times mol}\right]$
F	Faraday constant $\left[\frac{C}{electron\_mol}\right]$
$\overline{n}$	electron moles involved in the electrochemical process
E^o	open-circuit voltage (V)
b	Tafel slope (V)

a	electrode surface (cm^2)
i_o	exchange current density (A/cm^2)
R_e	electrolyte resistance (Ω)
$R(x)$	diffusion process resistance (Ω)

References

1. Srinivasan V, Newman J (2004) J Electrochem Soc 151:A1517. doi:10.1149/1.1785012
2. Andersson AS, Kalska B, Häggström L, Thomas JO (2000) Solid State Ion 133:41. doi:10.1016/S0167-2738(00)00311-8
3. Andersson AS, Thomas JO, Kalska B, Häggström L (2000) Electrochem Solid-State Lett 3:66. doi:10.1149/1.1390960
4. Yamada A, Chung SC, Hinokuma K (2001) J Electrochem Soc 148:A224. doi:10.1149/1.1348257
5. Prosini PP, Carewska M, Scaccia S, Pasquali M, Zane D, and Passerini S Proc. (2001) ECS 200th meeting, S. Francisco, September
6. Chung SY, Bloking JT, Chiang YM (2002) Nat Mater 1:123. doi:10.1038/nmat732
7. McKinnon WR, Haering RR (1987) Modern aspect in electrochemistry. Plenum, New York
8. Bisquert J, Vikhrenko VS (2002) Electrochim Acta 47:3977. doi:10.1016/S0013-4686(02)00372-9
9. Tarasenko NA, Tarasenko AA, Bryknar Z, Jastrabik L (2004) Surf Sci 562:22. doi:10.1016/j.susc.2004.06.143
10. Takahashi M, Tobishima S, Takei K, Sakurai Y (2002) Solid State Ion 148:283. doi:10.1016/S0167-2738(02)00064-4
11. Cowel Senft D (1996) Appl Surf Sci 231:94/95:235
12. Kortüm G (1968) Piccin (eds) Trattato di elettrochimica 1nd Padova
13. Bianchi G, Mussini T (1976) Tamburini, Masson (eds) Elettrochimica Milano
14. Ho C, Raistrick ID, Huggins RA (1980) J Electrochem Soc 127:343. doi:10.1149/1.2129668
15. Prosini PP, Zane D, Pasquali M (2001) Electrochim Acta 46:3517. doi:10.1016/S0013-4686(01)00631-4
16. Peña JS, Soudan P, Arean CO, Palomino GT, Franger S (2006) J Solid State Electrochem 10:1. doi:10.1007/s10008-004-0638-2
17. Montella C (2002) J Electroanal Chem 518:61. doi:10.1016/S0022-0728(01)00691-X
18. Montella C (2005) Electrochim Acta 50:3746. doi:10.1016/j.electacta.2004.12.035
19. Vorotyntsev MA, Levi MD, Aurbach D (2004) J Electroanal Chem 572:299. doi:10.1016/j.jelechem.2003.12.014
20. John Wen C, Boukamp BA, Huggins RA, Weppner W (1979) J Electrochem Soc 126:2258. doi:10.1149/1.2128939
21. Levi MD, Levi EA, Aurbach D (1997) J Electroanal Chem 421:89. doi:10.1016/S0022-0728(96)04833-4
22. Prosini PP (2005) J Electrochem Soc 152:A1925. doi:10.1149/1.2006607